



journal homepage: <http://civiljournal.semnan.ac.ir/>

Assessment of Damage and Residual Load Capacity of the Normal and Retrofitted RC Columns against the Impact Loading

S. Mollaei^{1*}, M. Babaei¹ and M. Jalilkhani²

1. Department of Civil Engineering, University of Bonab, Bonab, East Azerbaijan, Iran.

2. Engineering Faculty of Khoy, Urmia University, Khoy, West Azerbaijan, Iran.

Corresponding author: s.mollaei@ubonab.ac.ir

ARTICLE INFO

Article history:

Received: 09 March 2020

Accepted: 08 June 2020

Keywords:

Impact loading,

RC column,

Circular section,

Square section,

Steel jacketing,

Residual axial load capacity.

ABSTRACT

In the current study, the effect of the extreme lateral loading on the square and circular Reinforced Concrete (RC) columns with and without retrofitting was investigated. Retrofitting by the steel cage and steel jacketing was considered in this study. 3D finite element modeling of the columns and impact loading condition was performed using the ABAQUS/Explicit software. The data of a real scale blast test carried out in our previous study were used to verify the modeling accuracy. In these models, the effect of secondary moments ($P-\delta$) due to axial load, different geometrical characteristics of the steel jacket, varying compressive strength of the concrete material, and percentage of the longitudinal reinforcement on the explosive capacity of the column and its residual axial strength were studied. The main objective of this study was evaluating different explosive behaviors of the circular and square RC columns. Results showed that the circular columns perform better under the sudden lateral pressure than equivalent square ones. Also, steel jacketing increased the explosive capacity of the column, which was more effective in the circular columns than the square ones. The results also indicated that steel jacketing with less buckling capacity had the least improvements on the column capacity. It was found that the effects of the initial axial force in the column were significant on its behavior under explosive loading condition, which should be taken into account in any modeling approaches. In general, the $P-\delta$ phenomenon had less effect on the circular columns than the square ones. Also, the use of a high-strength concrete and a higher percentage of longitudinal reinforcement further influenced the retrofitted columns than unretrofitted (normal) ones, which was more evident in the circular columns in comparison with square columns.

1. Introduction

A wide range of engineering structures such as high-rise buildings, bridges, tunnels, dams, platforms, and security-military shelters are made of the reinforced concrete material. According to the review of technical literature, analysis and design of the RC structures under static and seismic loading have received a great deal of attention. However, since many structures may experience severe dynamic loads such as blast and impact loads during their lifetime, it is essential to investigate the behavior of Reinforced Concrete (RC) structures under blast loading.

Recently, numerous studies have been conducted on the effect of blast loading on the infrastructures. These studies have focused on the extent of damage and the behavior of structures under this type of loading. Due to the complex behavior of the structures under the blast loading and post-blast conditions, the effect of the blast loading on the infrastructures is usually investigated at two scales: local damage of the structural members and global damage of the whole structure. Columns are the key load bearing members in the structures, and they are the first members of the structure to be mostly influenced by the lateral pressure loading in the case of an explosion event near the structure. Column failure is one of the most important causes of progressive collapse in the framed structures. Progressive collapse is the leading reason of deaths and injuries caused by the explosion events, and its damage could be far higher than the direct damage of the blast pressure [1-3].

Recently, empirical studies have been carried out on a variety of RC structures including RC columns, against blast loading [4-7].

Given the complexity, difficulties, limitations, and high cost of the laboratory research in this field, analytical studies and software modeling can be good alternative to laboratory methods. Finite Element Method (FEM) is a powerful tool to estimate the behavior of structures under the blast loading with a reasonable accuracy without the high cost and difficulties of the explosion tests. Shi et al., [8] proposed a failure criterion based on the residual axial load capacity for RC columns using the numerical modeling by the LS-DYNA software. They plotted the PI (Pressure-Impact) diagrams for the column based on this failure criterion [8]. Bao and Li [4] carried out the parametric studies on RC columns under the blast loading using the numerical modeling on the LS-DYNA hydrocode. Wu et al., [9] conducted a similar research using the Arbitrary Lagrangian Eulerian (ALE) method in the LS-DYNA software to analyze the response of the columns under the contact explosion. Roller et al., [10] studied the residual resistance of a series of small-scale circular RC columns. Astarlioglu and Krauthammer [11], as well as Aoude et al., [12] investigated the UHPFRC¹ columns under the idealized blast loading.

In addition to the LS-DYNA [13], which is a specialized tool for modeling the structures under the blast loading, the ABAQUS/Explicit [14] finite element software has also been successfully used to simulate the RC structural members under the blast loading [15]. Arlery et al., [16] used the ABAQUS/Explicit software in finite element modeling to investigate the effect of the very close explosions on the RC columns. In this study, the explosion center was very close to the structure where the structural

¹ Ultra-High Performance Fiber Reinforced Concrete

response was often localized and presented in the form of the erosion in the section. They validated the blast loading results of the RC column using the CONWEP module [17] in the ABAQUS/Explicit software by the Eulerian hydrocode OURANOS analyzer. In this paper, ABAQUS/Explicit software is used for modeling and analyzing the considered columns under the blast loading.

Some researchers have focused on retrofitting and strengthening the RC columns under the blast loading. Crawford [7] studied the methods of using the Fiber-Reinforced Polymer (FRP) coatings to enhance the strength of RC columns under the simultaneous blast and axial loads. Carriere et al., [18] introduced the Steel - Reinforced Polymer (SRP) coatings as a suitable replacement for Carbon Fiber - Reinforced Polymers (CFRPs) to strengthen the RC members under the blast loading. Most of these studies have focused on the FRP coatings, and other explosive strengthening methods have not been addressed.

Retrofitting with steel jackets and steel cages is a common approach to increase the strength of the RC members, which is accompanied with advantages such as high effectiveness, low cost, and ease of execution [19,20]. Therefore, there is a need to investigate the effectiveness of this type of retrofitting in improving the behavior of RC columns. Crawford et al., [21] used the numerical modeling in the DYNA3D software to investigate the effect of steel cylindrical coatings on the explosive capacity of the RC columns. Thai et al., [22,23] investigated the retrofitting of the RC square columns under the blast loading using steel sheets and LS-DYNA software. They only considered one type of retrofitting and called

it Steel Confined Reinforced Concrete (SCRC). In some studies, explosion tests have been carried out on the steel jacketed RC columns with circular [24, 25], square, or rectangular sections [26-29]. In some cases, unfortunately, there is no public access to the blast test data because of national security concerns.

Crawford et al., [21] conducted one of the first blast test studies on the retrofitted RC columns. Thai et al., [23] evaluated the effect of the steel jacketing of RC column using the FE modeling. They presented some discussions and recommendations on the blast performance of steel-jacketed columns. Fouche et al., proposed a modified steel jacketing [24] to provide the blast resistant RC bridge columns. All the relevant researches have only addressed fully wrapped columns using the steel covers. So, there is still a need to investigate other possible types of steel jacketing.

Studies on the RC columns under the blast loading showed that most cases have been conducted without considering the retrofitting effects. Also, only the use of polymer sheets has been considered in most studies done in the field of retrofitting the RC columns under the blast loading. On the other hand, further investigations are required in this area due to the uncertainties in the explosion phenomenon and the complexity of the behavior of RC sections under the lateral blast loading conditions.

In this paper, three-dimensional models of the RC column with and without retrofitting were investigated under the blast loading. The blast test results performed in our previous study (Esmaeilnia and Mollaei, 2017) [30] were used to validate the developed finite element models. Also, the

effects of changes in the geometric pattern of the steel jacketing, the percentage of longitudinal steel, the compressive strength of the concrete, and the initial axial load applied to the column were investigated on the damage and residual axial load capacity of the square and circular RC columns. Thus, the main objective of the present paper is investigating the different effects of the same steel jacketing on the circular and square RC columns under blast loading. It is assumed that the shape of the column may change the retrofitting efficacy. Hence, the possible differences are also studied.

2. Numerical Modeling

2.1. Considered RC Column Models

Herein, two types of RC columns with square and circular cross-section were considered. For square cross-sections, RC columns were used with the specifications provided by Belal et al., [31], and the circular columns had the cross-sectional area and steel reinforcement similar to the square cross-sections. Six models of RC columns included one simple column (without retrofitting) and five columns retrofitted by different steel jackets. Fig. 1 and Table 1 present the cross-sections and geometrical details of retrofitting for all the specimens. Square columns had a cross-section with 200 mm of diameter; circular columns had 226 mm of diameter, with 1200 mm of height and same reinforcement. In this study, retrofitting designs were originally developed aimed at increasing the axial load capacity of the columns under static axial loading [31]. The components used in retrofitting the specimens were selected in a way that they all had the same horizontal cross-sectional area [31]. Regarding naming of the models, letter C represents the column, M stands for

the square section, D denotes the circular section, and the numbers 1 to 6 refer to the types of steel jacket retrofitting (number 1 means simple column without strengthening).

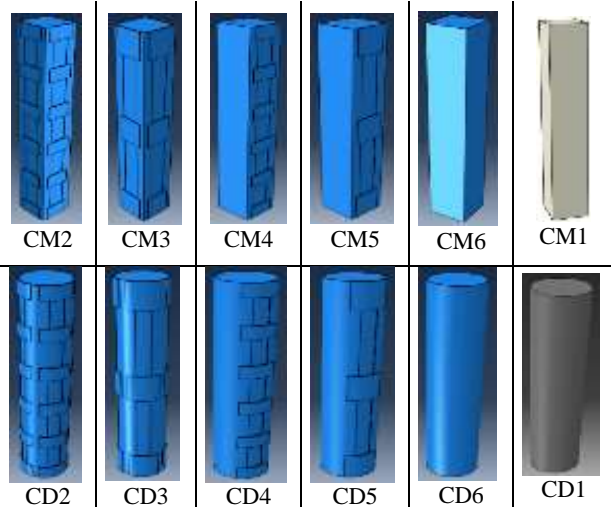


Fig 1. Details of dimensions and retrofitting of the RC columns

Table 1. Model specifications (dimensions: mm)

Model	Strengthening configuration	Reinforcement	Dimensions (mm)
CM1	No- strengthening	4 ϕ 12 ϕ 8@100	□ 200×200× 1200
CM2	steel angles- 4 L 50×50×5 + 3×4 plates 150×100×2		
CM3	steel angles- 4 L 50×50×5 + 3×4 plates 150×50×2		
CM4	steel channels- 2C (206×50)/(3.1×3.1)+ 3×4 plates 150×100×2		
CM5	steel channels- 2C (206×50)/(3.1×3.1)+ 3×4 plates 150×50×2		
CM6	Complete steel jacket (steel plates) 4×4 plates 200×2.4		
CD1	No- strengthening	4 ϕ 12 ϕ 8@100	○ 200×200× 1200
CD2	Curved steel sheet - 4 95×5 + 3×4 plates 150×100×2		
CD3	steel angles- 4 95×5 + 3×4 plates 150×50×2		
CD4	C-shaped steel channels- 2C (295×4) + 3×4 plates 150×100×2		
CD5	C-shaped steel sheet- 2C (295×4)+ 3×4 plates 150×50×2		
CD6	Complete steel sheet cover (t=3)		

Table 2. Steel material specifications

Steel Rebars	E_s (MPa)	F_y (MPa)	F_u (MPa)	Failure strain
Longitudinal bars	210000	360	463	11
Stirrups	210000	240	340	14

Table 2 presents the properties of steel material, where the failure strain is the strain corresponding to the ultimate tensile stress of the steel. The average compressive strength of concrete was equal to 35 MPa, and its density was equal to 2400 kg/m³. Four longitudinal AIII rebars with 12 mm diameter were used for longitudinal steel, and closed stirrups with diameter of 10 mm were placed at specified intervals throughout the column height. Both ends had a fixed support condition in all the 12 specimens. The upper end of the columns exposed to the axial gravity load had a displacement degree of freedom in vertical direction.

Usually, the value of the initial axial load in the columns behavior of which is investigated under the blast loads is defined as a proportion of the nominal axial resistance of the column ALR² Equation (1). According to the practical examples, ALR is usually within the interval of 0.1 - 0.4 [4,8,32].

$$ALR = \frac{N}{N_{max}} \tag{1}$$

Where, N_{max} is the nominal axial load capacity, and N is the axial force applied to the column.

2.2. Concrete Material Model

In this study, the Concrete Damage Plasticity (CDP) model was applied that was introduced by Lubliner et al., [33] and was further refined by other researchers to model

the behavior of the concrete [34, 35]. In this model, two main concrete failure mechanisms of tensile cracking and compressive crushing were assumed. Nonlinear concrete behavior was described using the isotropic damage plasticity and tensile and compressive elasticity. Fig.2 shows the stress-strain diagrams of the concrete in uniaxial tensile and pressure conditions.

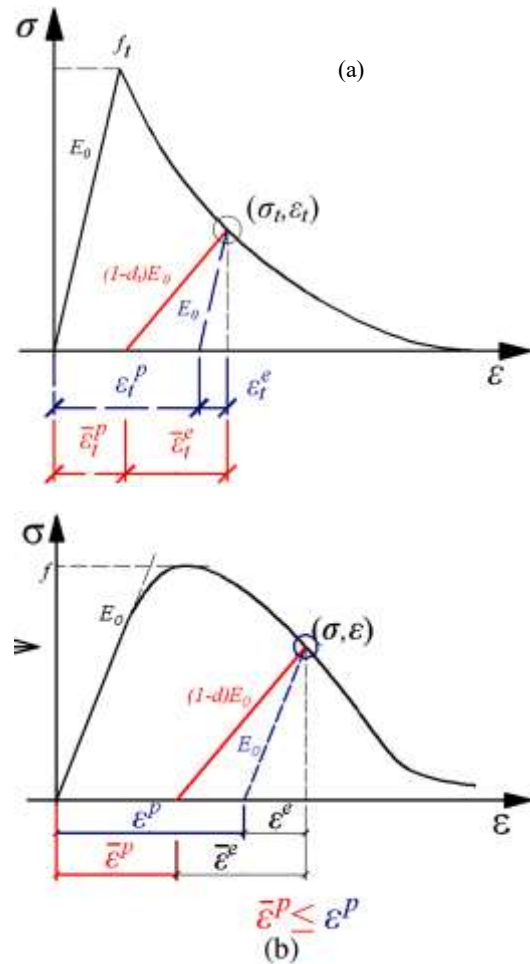


Fig 2. Uniaxial behavior of the concrete in: (a) tension and (b) pressure.

As shown in Fig. 2, E_0 represents the modulus of elasticity, ϵ_t^{ck} is the cracking strain, ϵ_t^{in} represents the non-elastic strain corresponding to the stress, and d_t and d_c are the tensile and pressure damage parameters,

² Axial Load Ratio

respectively. Completion of the fracture level was controlled by the hardening variables ε_c^{pl} and ε_t^p related to the failure mechanisms under compressive and tensile loads [14]. ε^{pl} and ε^{pl} are the corresponding plastic strains, respectively. The stress-strain curve changes linearly with respect to the failure stress point σ_{t0} due to the uniaxial tension, which is associated with the onset and extent of the micro cracks in the concrete. After passing this point, the failures turn into the visible cracks as represented by the softening curve in the stress-strain space. The response will be elastic under uniaxial pressure, until it reaches the σ_{co} yield point, and the behavior in the plastic zone is generally expressed as a hardness curve. Eventually, the curves turn into the softening curve at the final stress point σ_{cu} [14].

The William-Warneck failure criterion and the Hillborg fracture energy were used to describe the failure and propagation of the concrete cracks in the CDP model. The general form of this criterion is a cone-like shape in the stress space. Each stress state corresponds to a point in the stress space. If this point is outside the defined space of the relationship, it will represent the failure of the material [14]. In the Hillborg fracture energy model, the brittle behavior of the concrete is characterized by the stress-displacement response rather than the stress-strain response under tension. The crack fracture energy model can be obtained by expressing post-fracture stresses as a function of crack width [14].

In the CDP model, the values of dilation angle, eccentricity, f_{b0} / f_{c0} ratio (biaxial compressive stress to uniaxial compressive stress), yielding parameter k , and viscosity parameter μ were equal to 40, 0.1, 1.16, 0.6667, and 0.001, respectively.

2.3. Steel Material Model

In this study, for modeling the steel material, the elastic-perfectly plastic constitutive model was assumed with linear elastic behavior before reaching the yield stress followed by the plastic behavior until development of the failure stress. Herein, the Von-Mises yield point was used for steel material, assuming that yielding is a function of the principal stresses occurring when the stress point in the space of the principal stresses reaches a critical value (Eq. 2).

$$\phi = \frac{1}{2} [(\sigma_1 - \sigma_3)^2 + (\sigma_1 - \sigma_2)^2 + (\sigma_2 - \sigma_3)^2] - F_y^2 \quad (2)$$

Where, ϕ represents the stress state of the point, σ_1 , σ_2 , and σ_3 denote the principal stresses, and F_y is the yield stress. The above equation defines a three-dimensional space where each stress state corresponds to a point in the stress space. If this point is outside the three-dimensional cylinder described above, the material will yield. This model does not include the hardening effects [14].

Besides, the interaction between concrete and rebar is a critical parameter in modeling the RC material. This interaction causes the stress transfer between the two concrete and steel parts and their interconnection. In this study, the embedded element model was used to model the interaction between the concrete and steel. In this technique, if a node of steel elements is placed between the concrete elements, the Degrees of Freedom (DOF) of that node are eliminated and the node becomes embedded. Thus, the DOFs of the embedded node are calculated by the DOFs of the concrete nodes adjacent to that embedded node. The number of DOFs in each embedded node depends on the DOF of the adjacent concrete node [14].

2.4. Mesh Sensitivity Analysis

The solid C3D8R element was used for 3D modeling of the concrete. It is a three-dimensional cubic element with eight nodes that uses the reduced integration method. Truss type T3D2 element was used for modeling of the rebars, which is a three-dimensional truss element with two nodes. For modelling the steel jacket, the S4R shell element was used, which is a 4-node 3D shell element with 6 DOF per node [14].

Meshing sensitivity analysis was performed to obtain optimum dimensions of the mesh with acceptable accuracy and reasonable computation time. Herein, as shown in Figs. 3 and 4, the size range of 15-80 mm was selected for the mesh with 5 mm increasing steps. The column capacity value was determined for each mesh size. There was a slight difference in the results up to the size of about 40 mm, and it was more significant for larger mesh sizes. As a result, a size of 40 mm was chosen for meshing the models. The analysis time of the models increased significantly at 25 mm of mesh size while, the difference in computational results was about 3 - 5%. Fig. 5 shows a model of the meshed column.

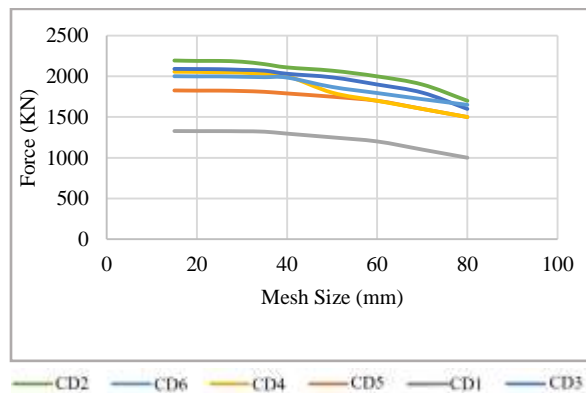


Fig 3. Mesh sensitivity analysis on the circular columns

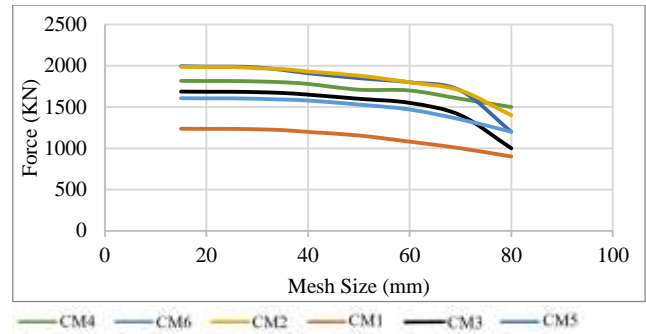


Fig 4. Mesh sensitivity analysis on the square columns

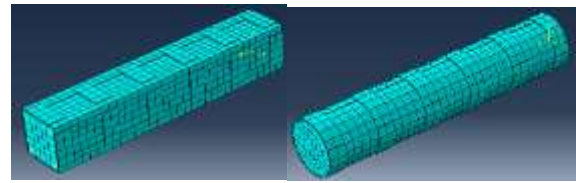


Fig 5. An example of the meshed column

2.5. Blast Loading

The explosion event occurs as a result of the sudden release of large amounts of light, heat, noise, and pressure waves created around the center of the explosion. Part of the energy generated by the blasting is released by heat radiation, and the other part enters the air (air blast) and the ground (ground shock) by the radial waves [36]. Fig. 6 presents the approximate pressure-time diagram at a certain distance from the center of the explosion. As can be seen in Fig. 6, the time A corresponds to the moment before the arrival of the wavefront, and the moment B occurs after the shock hits indicating a sudden increase of pressure. At the moment C, the positive pressure ends, and the negative phase (i.e., suction) of the pressure can be felt. Time D is related to disappearance of the effects of the explosion wave and return of the ambient pressure to normal pressure [37].

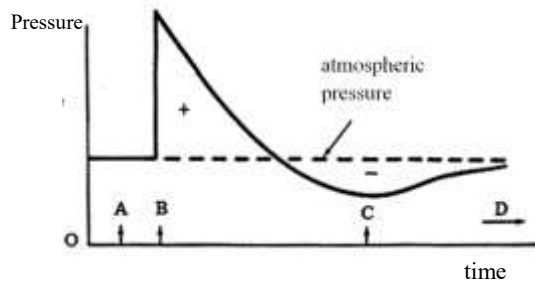


Fig 6. Pressure-time diagram of the blast wave

Due to the terrorist attacks, explosions are most likely to occur at distances close to the structure with the smallest amounts of explosives followed by the explosions with higher amounts of explosives at farther distances [38,39]. Since small amounts of explosives are easier to prepare and it is easier to hide small and light packages, there is always a high possibility for occurrence of deliberate explosions with low amounts of explosives. Herein, the blast loading refers to this particular type of intentional or unintentional explosive event.

Blast loading can be performed directly (experimentally) in the ABAQUS software based on the UFC 3-340-02 recommendation [37] or can be directly applied through the CONWEP [17] module in the ABAQUS software. According to the literature [36], the following equation $Z = \frac{R}{W^{1/3}}$ was provided to determine the scaled distance, where W is the equivalent charge weight of TNT, and R is the standoff distance. In the experimental method, according to Z value, the amount of explosion-induced reflection pressure and its continuation time are estimated based on the UFC 3-340-02 recommendation, and the resulting pressure-time diagram is introduced to the software by the user. Besides, various studies have presented the methods for estimating the temporal and spatial distribution of the pressure resulting from the explosion on the structure [36, 37, 40-41].

In the CONWEP method, the point of blast center location is defined as well as the interaction surface of the blast pressure on the structure. Then, the blast pressure time-history applied to the structure is calculated by applying the amount of charge weight and specifying the type of wave propagation (surface, spherical, etc.) using the software. In this paper, the latter method was used for blast loading of the models. In the CONWEP method, the face of the column is defined as the interaction surface of the blast wave (Fig. 7). Herein, the explosion center was located at 2 m from the column mid-height node with a charge weight of 60 kg-TNT. This blast loading scenario had a scaled distance of $Z=0.51 \text{ m/kg}^{1/3}$ falling into the near-field range [42], which is a highly probable explosion event for building structures.

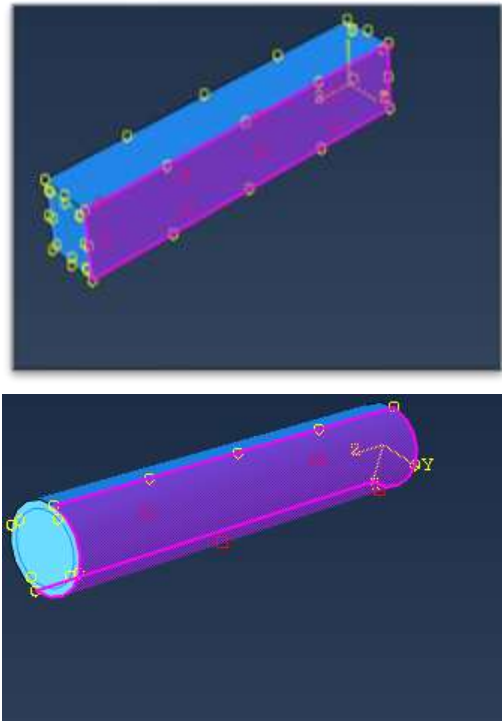


Fig 7. Definition of the blast wave interaction surface

Analysis procedure included the three steps of preloading, dynamic analysis (blast

loading), and post-blast capacity assessment. All the steps were implemented using the ABAQUS Explicit calculations. Axial force was gradually applied on the top of the column in the preloading and post-blast stages. The static response of the column was evaluated by a quasi-static ABAQUS Explicit calculation with a sufficient step time (more than 60 msec). The dynamic analysis under blast loading was implemented during 50 msec, which is a sufficient step time to subside the dynamic response (nodal velocities were vanished). Step time durations were selected according to the recommendations in the literature [43].

2.6. Verification of the FE Modeling

Firstly, the modeling and analysis process used in this study need to be validated to analyze the underlying models using this process. For validation of the finite element model of the RC column, the test results known as 0C0 were selected from a previous study [44]. The geometrical and reinforcement properties of this specimen were similar to those of the previous study. Fig. 8 shows specification of this model and its test procedure under axial static load. The compressive strength of the concrete in this specimen was equal to 79.5 MPa, and the yield stress of longitudinal and transverse bars was equal to 564 and 516 MPa, respectively [44].

The 0C0 column specimen was subjected to static axial loading according to the study by Hadi and Widiarsa, and the axial load-displacement diagram was plotted. For a better comparison of the results, the diagrams obtained from FE modeling and experiments were plotted together (Fig. 9). As demonstrated in Fig. 9, the results obtained from the FE method are consistent with the

experimental results with a good accuracy. Therefore, the FE method can be used in this research for further analyses.

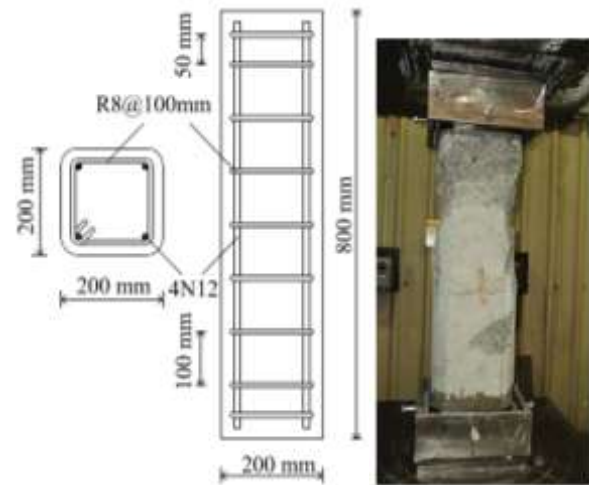


Fig 8. Example of the column used for validation [44]

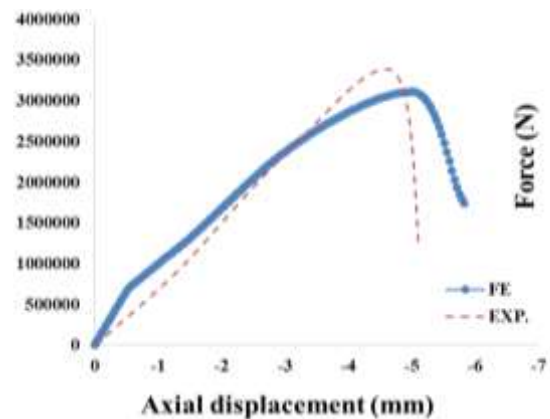


Fig 9. FE analysis results (bottom); blast test results [44] (top)

In the following, the results of the blast test performed in the study by Esmailnia Omran and Mollaei (2017) [30] were used to verify the blast analysis procedure. It should be noted that the mentioned study is a report of the investigations carried out by the same authors alongside this study [30]. Four similar concrete cross-section specimens were subjected to real blast loading test. Two RC samples had no axial force, and two of them had initial compressive axial pressure

using the post-tensioning method. Fig. 10 illustrates the profile of the specimen under the blast test and the support structure constructed in the test setup. Further details of this experiment have been reported in the literature [30, 45].

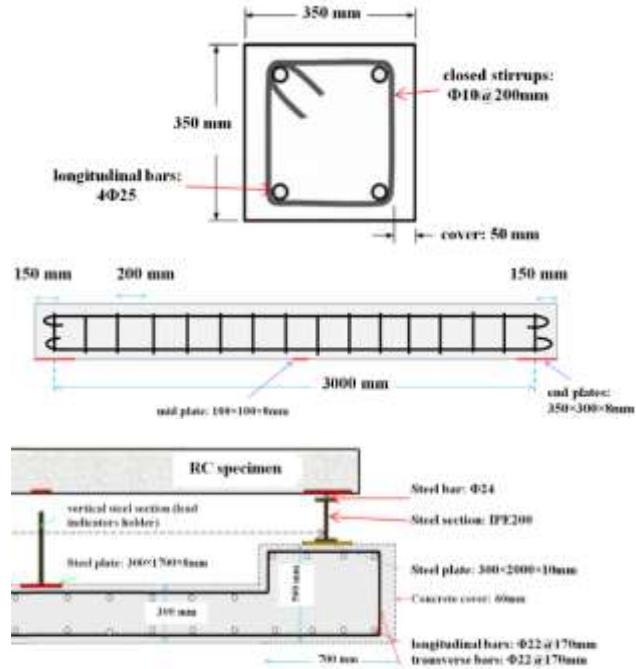


Fig 10. Details of the blast test setup [30]

Fig. 11 illustrates the axial strain diagrams recorded in the longitudinal bars in the front and back faces. The results of FE analysis were also plotted in the same diagrams. As can be seen in Fig.11, in all the models (with and without axial force), the FEM estimations are in a good agreement with the data recorded in real-scale experiments.

3. Results and Discussion

In this section, different column models are analyzed under the desired blast loads using the modeling process and FE analysis described in the previous sections. Figs.12 and 13 show deformed square and circular columns and steel jackets. Deformation

patterns in the steel jackets observed in this study are similar to those reported in the study by Crawford et al. [21].

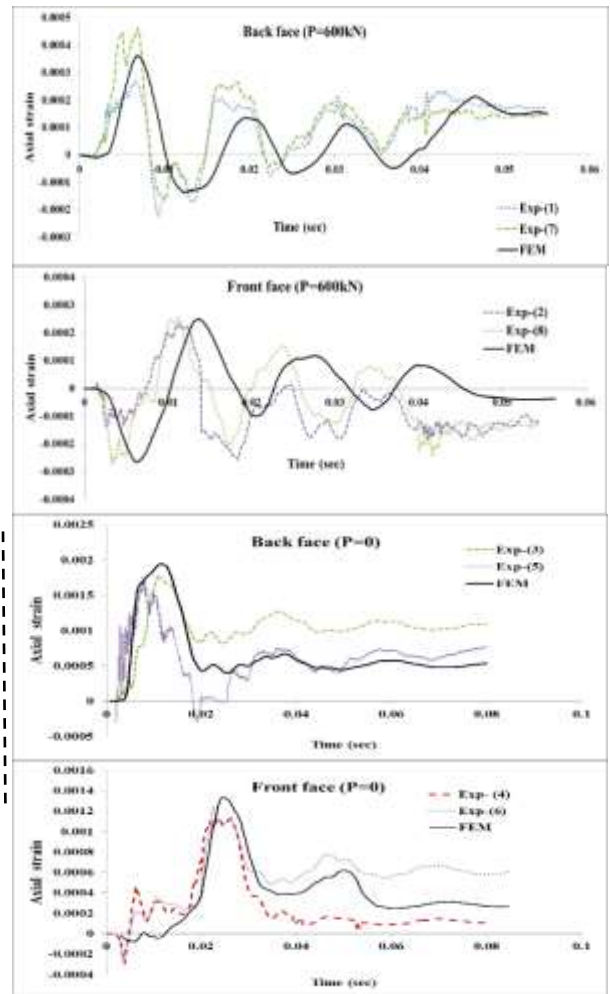


Fig 11. Axial strain-time curves for the longitudinal bars: experimental data [30] and FEM

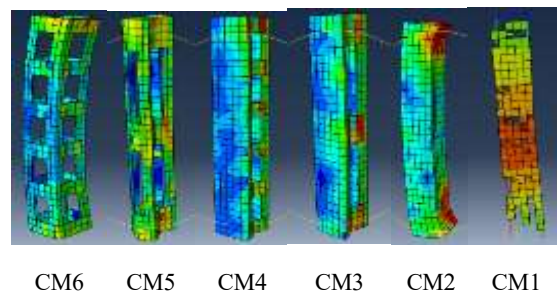


Fig. 12. An example of the deformation of square models under the blast loading.

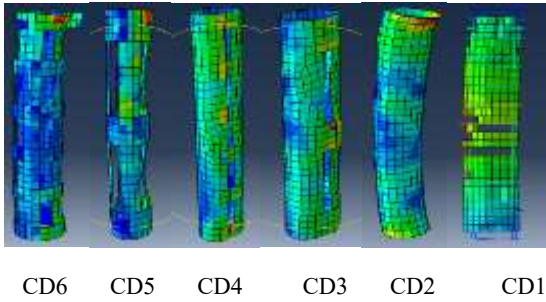


Fig. 13. An example of the deformation of circular models under the blast loading

Fig. 14 shows a graphical representation of the Von-Mises stress contours for square columns under the blast loading. As shown in Fig. 14, the CM2 model with three connecting strips exhibits more bending deflection than the CM3 model with six connecting strips. As the columns are fixed at both ends, the lower and upper ends of the column are more critical. For example, in the CM4 and CM3 models, the middle sheet experienced smaller Von-Mises stresses, and the sheets near the support had a critical stress state.

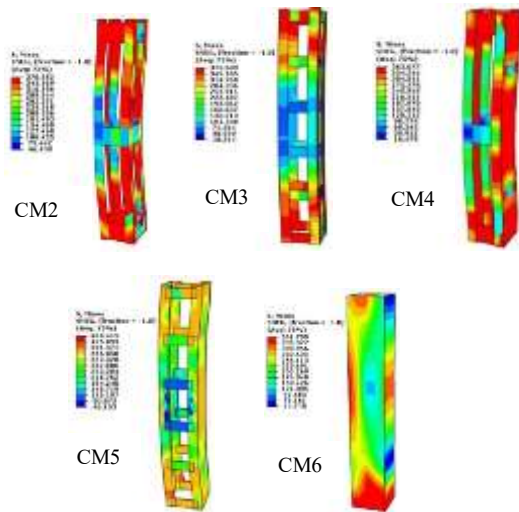


Fig. 14. Stress contours in the steel jackets

Fig. 15 shows the lateral displacement difference at the center of the height for the circular and square columns. The pairs of CM5-CD5 and CM6-CD6 columns had the largest lateral displacement difference of

about 8 mm, and the columns (CM1-CD1) had the least amount of displacement difference. The behavior of the RC columns with square sections under the blast loading was different from the circular columns. It can be stated that, this difference is even more evident in the retrofitted columns, even if similar steel jackets are used for them.

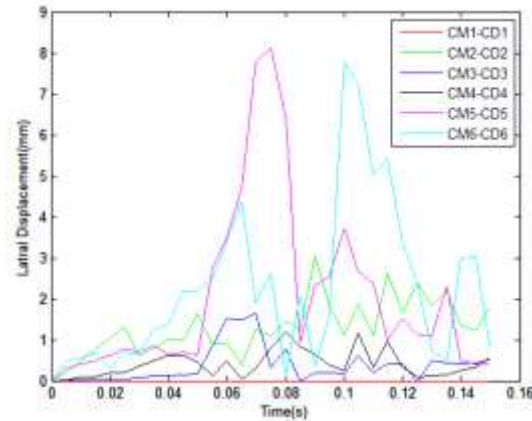


Fig. 15. Lateral displacement difference between circular and square column models.

3.1. Effect of the Concrete Compressive Strength

As shown in Figs. 16 and 17, the lateral displacement decreased by increasing the concrete compressive strength (f_c). For each 10 MPa increase in the compressive strength of concrete in the circular columns, lateral displacement decreased by approximately 11%, and in the square columns, it reduced by about 9%. Figs. 18 and 19 show the lateral displacement for all the specimens with different f_c values. As illustrated in Figs. 18 and 19, in both circular and square columns, type 4 retrofitting strategy has the largest reduction in the lateral displacement. The simple circular and square columns (CD1 and CM1) had the least reduction in the displacement. Therefore, it can be stated that, the use of a steel jacket increases the effect of concrete compressive strength on the explosive behavior of the column. This

probably occurs due to the increased effects of the concrete confinement.

The above-mentioned results confirm the blast design recommendations implying that the retrofitting wraps (like steel jacketing) protect the RC column against spalling and provide further confinement [42].

3.2. Effect of the Initial Axial Load

Figs. 20 and 21 illustrate the axial load versus axial displacement curves for circular and square columns with and without considering the P- δ effects. As can be seen in Figs.20 and 21, the capacity of the circular and square columns decreases by applying the effect of the P- δ phenomenon. Moreover, the column showed its maximum axial load capacity at a lower displacement than the case where the P- δ phenomenon was not considered.

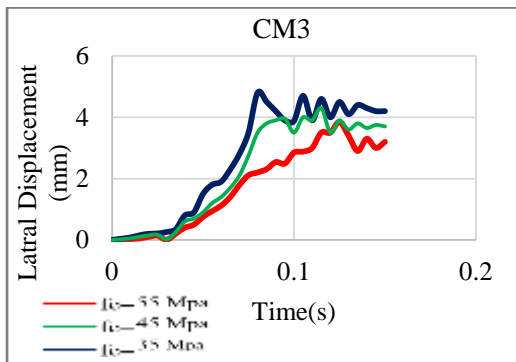


Fig 16. Lateral displacement at different f_c in CM3

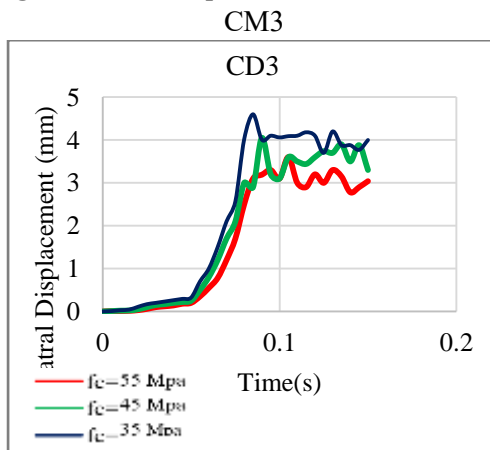


Fig 17. Lateral displacement at different f_c in CD3

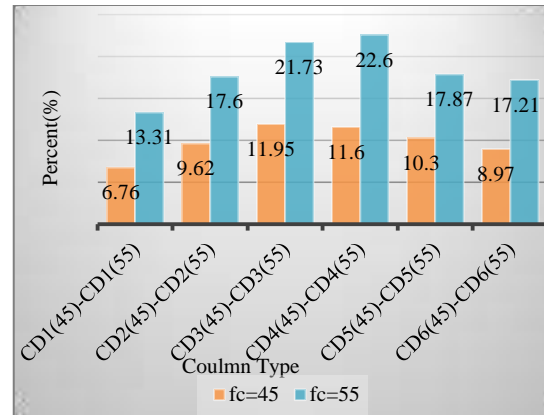


Fig 18. Decrease in the lateral displacement due to the increased f_c in the circular columns

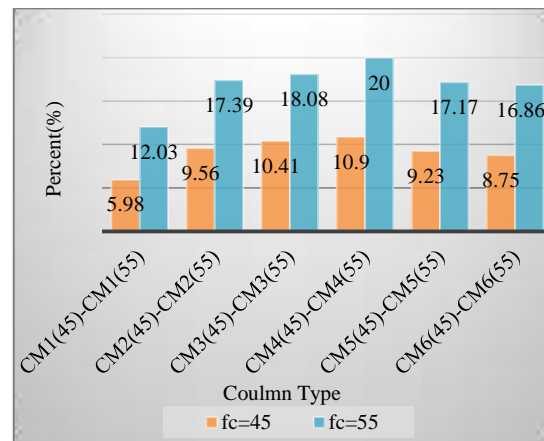


Fig 19. Decrease in lateral displacement due to the increased f_c in the square columns

Fig. 22 shows the reduction percentage of capacity considering the effect of P- δ on the circular and square columns under the blast loading. As depicted in Fig.22, the capacity reduction in the circular columns CD4 and CD3 is equal to 10 and 9%, respectively and for the square columns CM4 and CM3; it is equal to 15 and 14.8%, respectively, indicating that these two types of retrofitting (i.e., the use of narrow and wide-sided strips) perform better than other types of retrofitting configuration in the circular and square columns. Next, the complete steel jackets and two-sided strips are the most effective in reducing the effects of the P- δ phenomenon.

without P- δ — P- δ effects

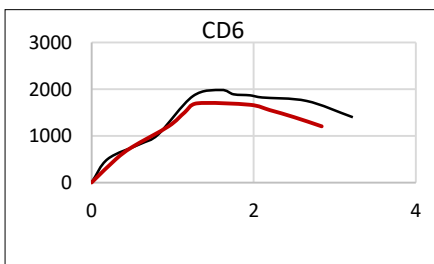
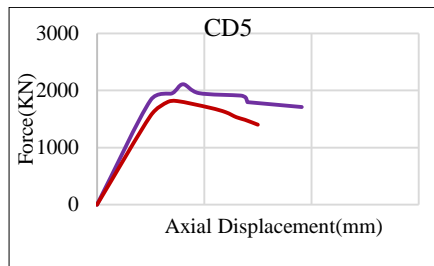
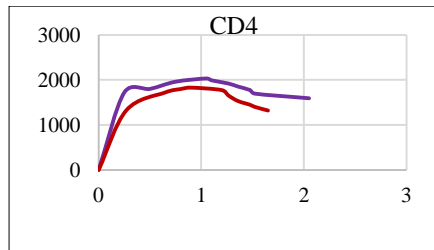
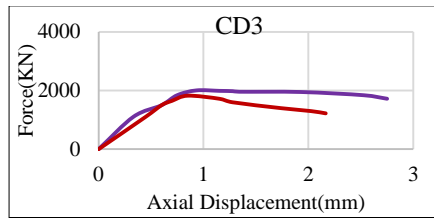
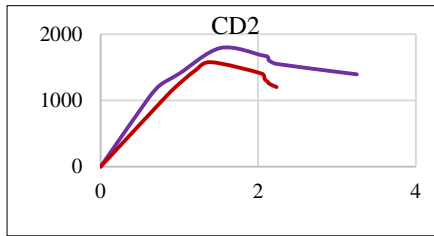
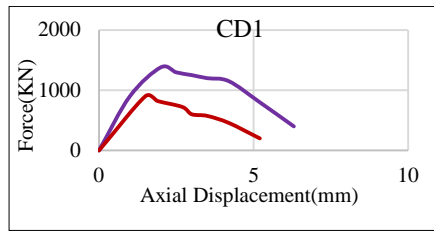


Fig 20. P- δ effect on the circular column

without P- δ — P- δ effects

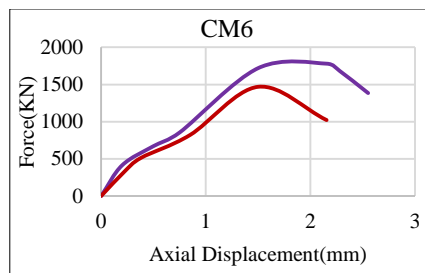
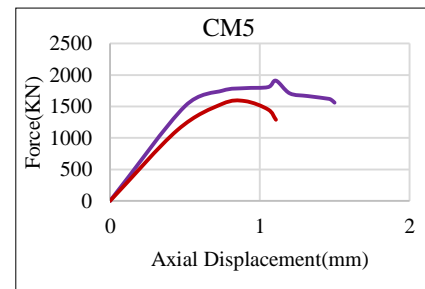
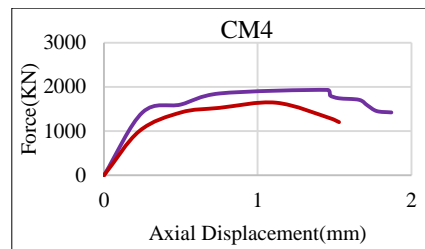
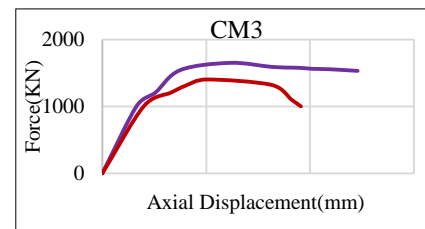
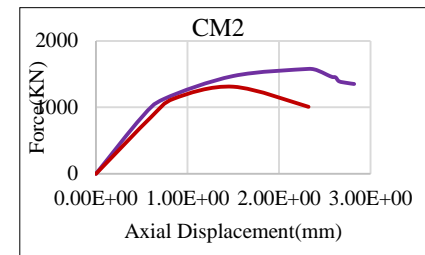
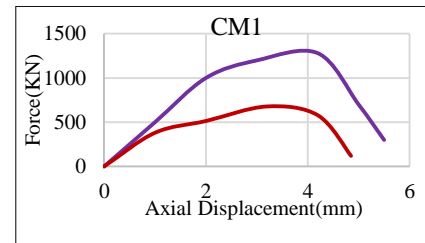


Fig 21. P- δ effect on the square column.

In the circular columns with the steel jacket, the capacity reduction due to P- δ phenomenon was less than the square columns; the capacity reduction of the retrofitted circular columns was between 10 - 15% and for the square columns, it was between 15 - 20%.

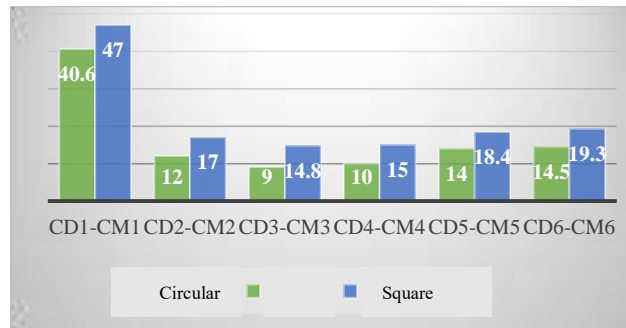


Fig 22. Capacity reduction due to the P- δ effects in the circular and square columns

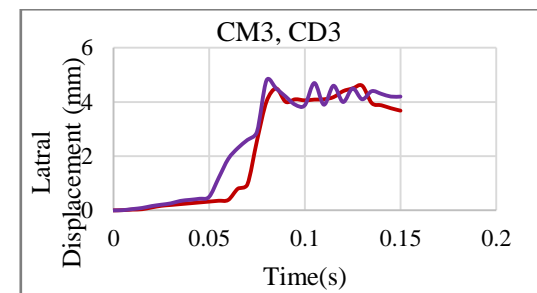
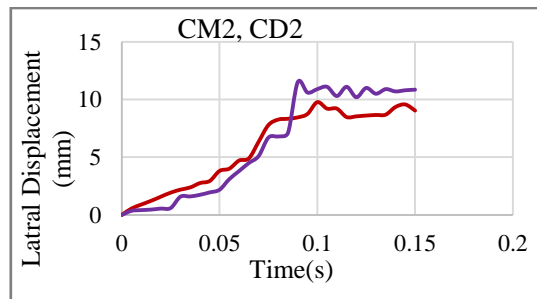
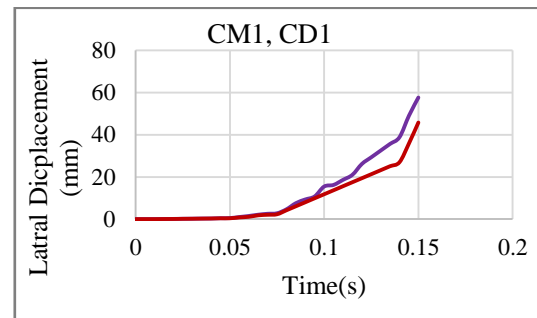
3.3. Effect of the Geometrical Properties of Retrofitting

Fig. 23 shows the lateral displacement diagrams of the square and circular columns with the same strengthening. As shown in Fig. 23, the behavior of the circular and square columns is brittle without retrofitting, and the lateral displacement of the column has increased abruptly. However, the columns retrofitted with steel jackets had higher flexibility. Circular and square columns with wide or narrow one-sided strip steel jackets had the highest explosive capacity because they had the least amount of deformation under the blast loading. This value was about 5 mm for a square column and approximately 4 mm for a circular one. One of the reasons for less displacement in the circular columns compared to similar square ones is the difference in their geometry. The loading surface under an explosion in a circular column is different from that of a square column, and this

geometric shape of the circular columns subsides the blast pressure through its edges.

As demonstrated in Fig. 23, a full (complete) steel jacket cannot be as effective as the other types of steel jacket in reducing the lateral deformation under the blast loading. As the sectional area of all types of the jackets is similar, the thickness of the overall steel jacket reduces. Angle profiles in the steel jackets are less effective in reducing the lateral deformation than other forms of retrofitting discussed in this study. This may be due to the severe deformation of different parts of the steel jacket with two-sided wide or narrow strips.

Square section — Circular section —



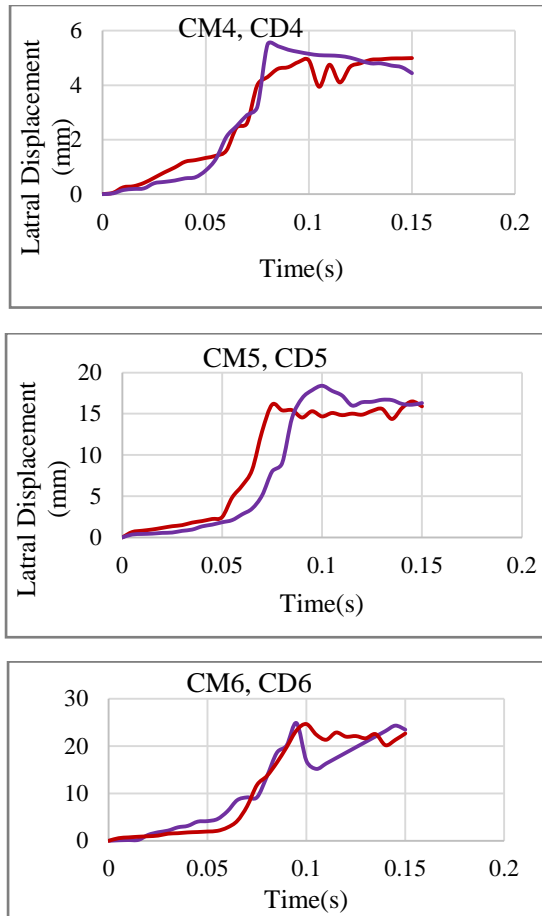


Fig 23. Lateral displacement of the circular and square column models under the blast loading

3.4. Effect of the Longitudinal Reinforcement

The rebars of the three models were meshed to investigate the deformation state of the steel bars under the effects of blast loading as shown in Fig. 24. As can be seen in Fig. 24, the bars in the CM4 model have a slight curvature resulting in high explosive capacity of the column. On the other hand, there is some plastic deformation in the bar grid of the CM6 model.

Figs. 25 and 26 indicate the lateral displacement time-history for different percentages of longitudinal reinforcement (0.01, 0.02, and 0.03%) in all the models. As shown in Fig. 25, the lateral displacement

decreases with the increase in the percentage of longitudinal steel. The decrease in the lateral displacement was about 8% for every 0.01% increase in the longitudinal steel for circular columns and it was approximately 5% for square ones. Among the circular columns, models CD3 and CD4 and among the square columns, models CM3 and CM4 had the highest reduction in the lateral displacement. Therefore, increasing the percentage of longitudinal steel to improve the explosive capacity of the column is more effective while using the steel jacket.

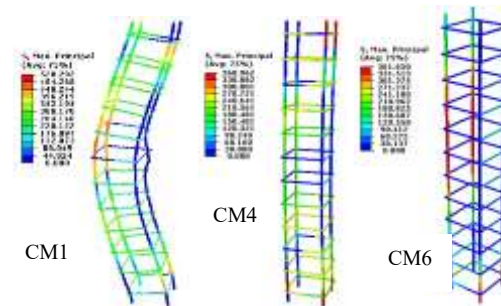


Fig 24. Curvature and deformation of the rebars in the CM1, CM4, and CM6 columns

3.5. Residual Axial Load Capacity

The axial load capacity ratio of the column after the explosion to its initial load capacity indicates the residual axial load capacity of the column. Knowing about the residual axial load capacity of the column can be useful in predicting the overall performance of the building, the progressive collapse process, and determining the stability of the building after the explosion experience, especially during the rescue missions. On the other hand, the residual axial load capacity is the best criterion to describe the extent of post-blast column damage [4, 16, 46]. Because, this criterion, unlike the maximum displacement or resistance criteria is independent of the behavioral modes of the structure.

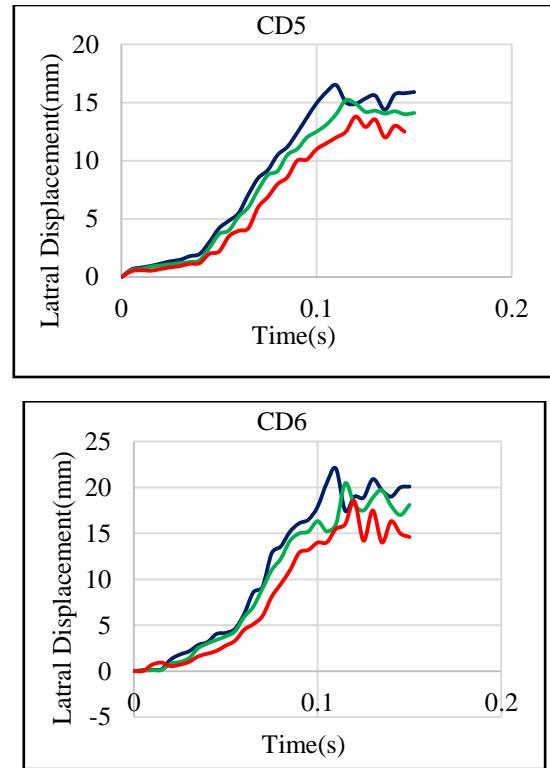
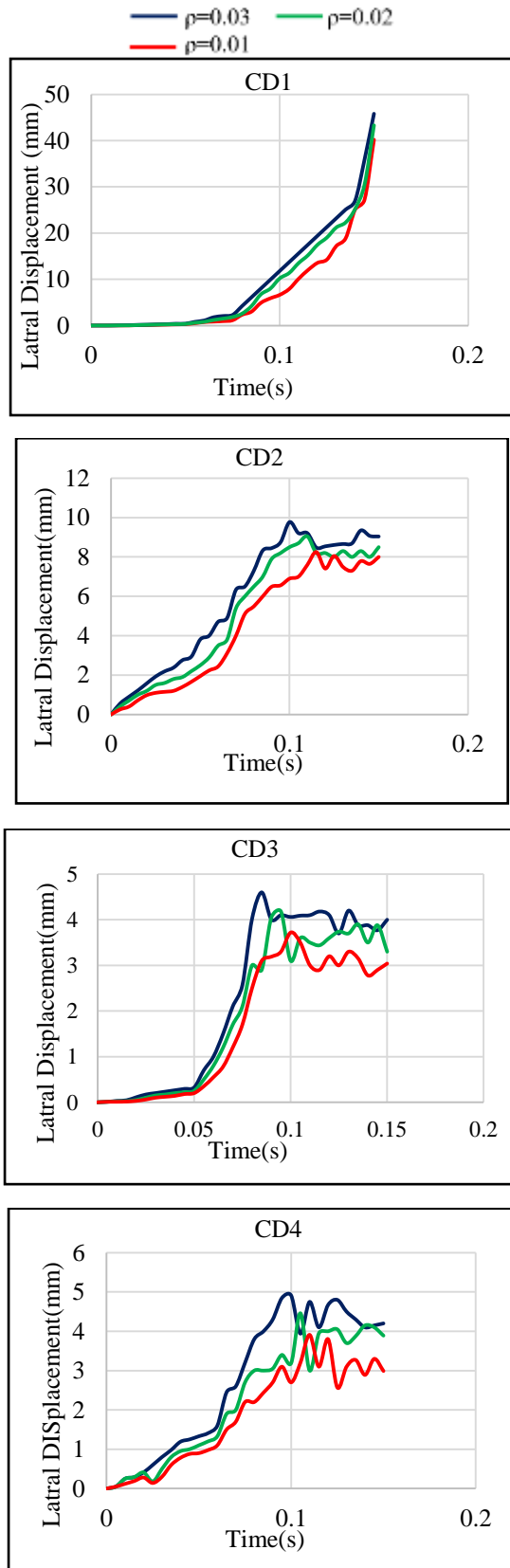


Fig 25. Lateral displacement for different percentage of longitudinal reinforcement ratio in the circular columns

In this paper, after the models were analyzed under the blast loading, a uniform compressive pressure was applied to the upper end of the column. The axial loading increased gradually and statically until the failure of the column. Fig. 27 shows the axial force versus axial displacement diagram (in a middle node at the roller end) for the square columns before and after the blast load experience (the letter P means post-blast). Fig. 28 shows the same diagrams for the circular columns.

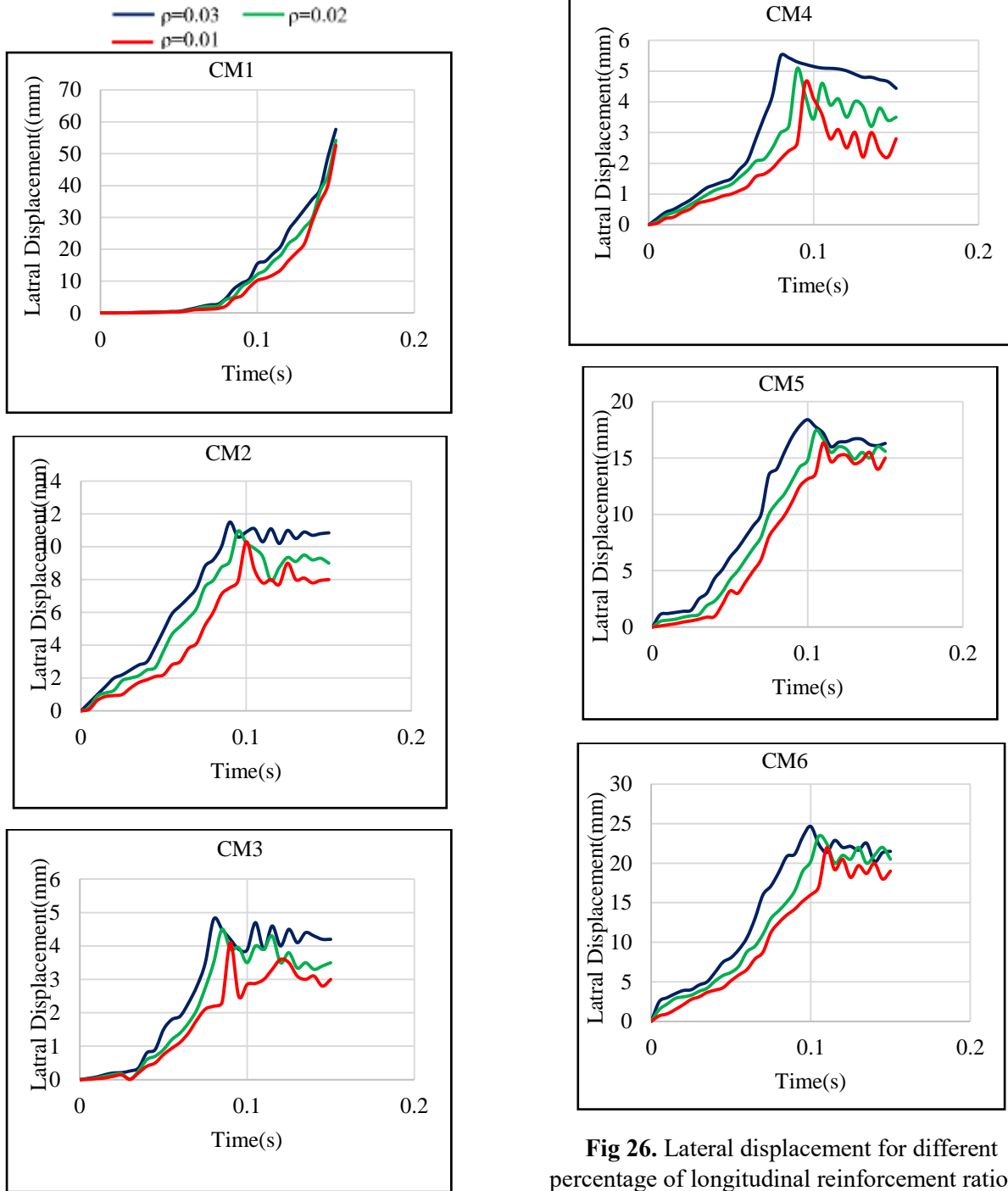


Fig 26. Lateral displacement for different percentage of longitudinal reinforcement ratio in the square columns

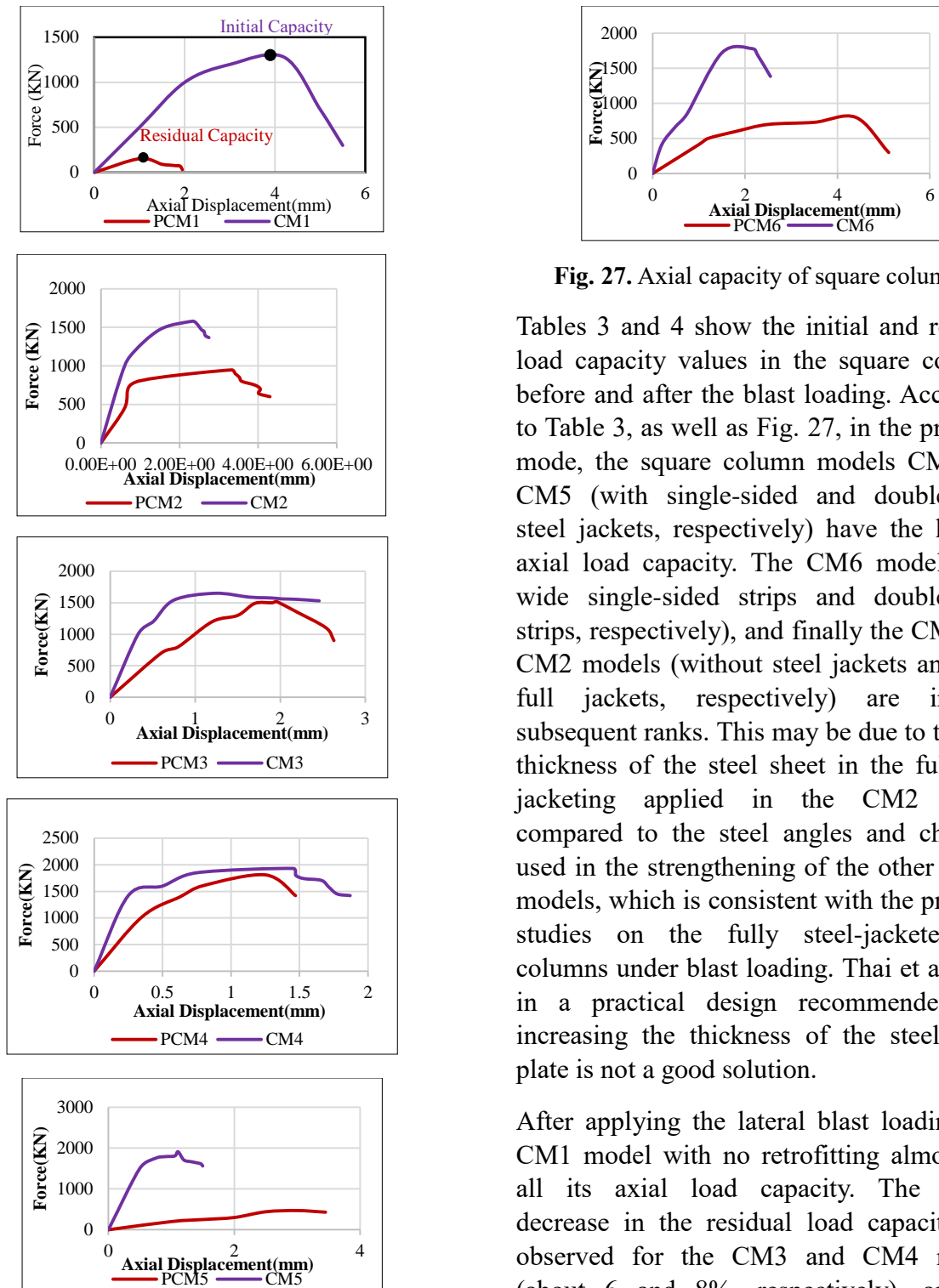


Fig. 27. Axial capacity of square columns.

Tables 3 and 4 show the initial and residual load capacity values in the square columns before and after the blast loading. According to Table 3, as well as Fig. 27, in the pre-blast mode, the square column models CM4 and CM5 (with single-sided and double-sided steel jackets, respectively) have the highest axial load capacity. The CM6 model (with wide single-sided strips and double-sided strips, respectively), and finally the CM1 and CM2 models (without steel jackets and with full jackets, respectively) are in the subsequent ranks. This may be due to the less thickness of the steel sheet in the full steel jacketing applied in the CM2 model compared to the steel angles and channels used in the strengthening of the other square models, which is consistent with the previous studies on the fully steel-jacketed RC columns under blast loading. Thai et al., [23] in a practical design recommended that increasing the thickness of the steel cover plate is not a good solution.

After applying the lateral blast loading, the CM1 model with no retrofitting almost lost all its axial load capacity. The lowest decrease in the residual load capacity was observed for the CM3 and CM4 models (about 6 and 8%, respectively), and the residual axial load capacity of the CM5 model significantly reduced (about 75%).

This significant reduction in the axial load capacity, which was also evident in the CM6

model (55%) could be due to the buckling of the angle profiles deformed by the lateral blast loading. Therefore, the steel jacket with one-sided strips had the highest increase in the explosive capacity of the column, and the double-sided steel jacket had the least improvement in the explosive capacity of the column. This may be due to the severe deformation of different parts of the steel jacket with the double-sided wide or narrow strips. This result could be influenced by shifting the position of the explosion center point. Herein, the explosion center was defined in front of the striped face of the column.

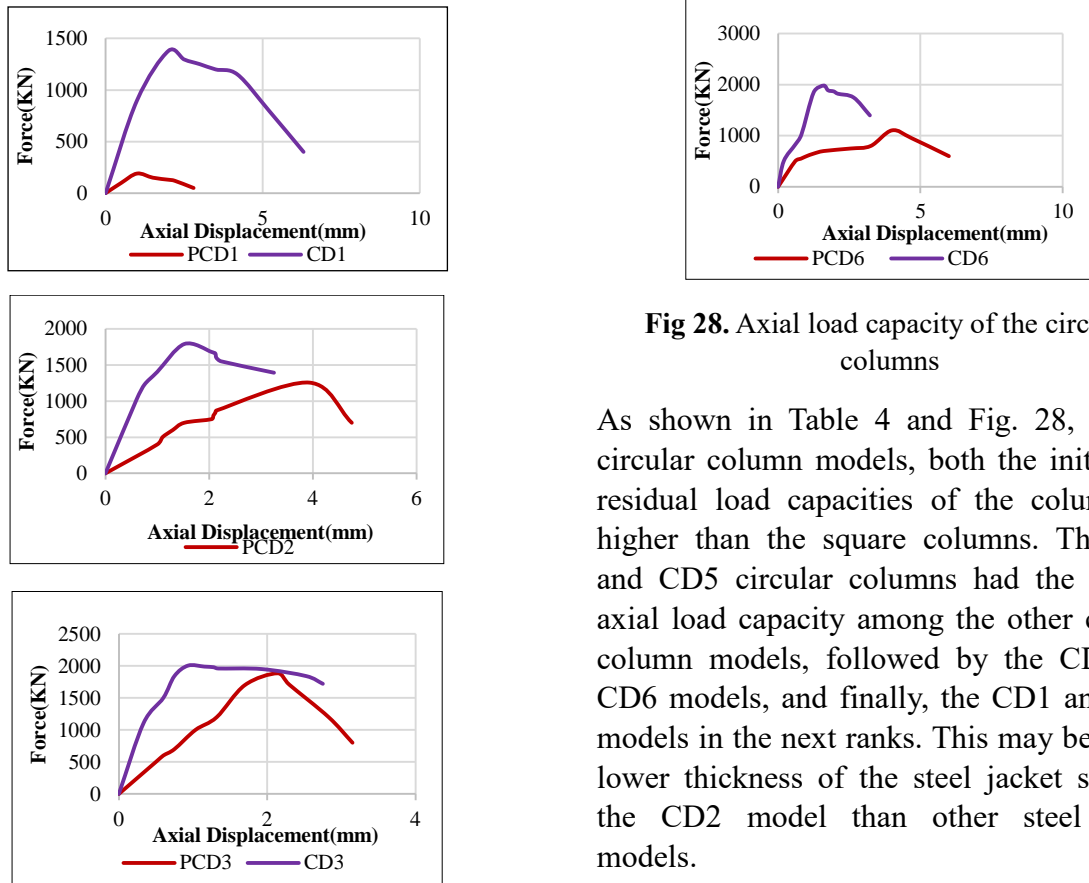


Fig 28. Axial load capacity of the circular columns

As shown in Table 4 and Fig. 28, for the circular column models, both the initial and residual load capacities of the column are higher than the square columns. The CD4 and CD5 circular columns had the highest axial load capacity among the other circular column models, followed by the CD3 and CD6 models, and finally, the CD1 and CD2 models in the next ranks. This may be due to lower thickness of the steel jacket sheet in the CD2 model than other steel jacket models.

After applying the lateral blast loading, the CD1 model with no retrofitting almost lost its axial load capacity under the blast loading. The lowest decrease in the residual capacity was observed for the CD3 and CD4 circular

columns (6 and 6.5%, respectively), and the residual axial load capacity of the CD5 model reduced significantly (about 60%). This significant reduction in the axial load capacity, also observed in the CD6 model (44%), maybe due to the buckling of the steel sheets deformed by the blast loading.

Given the capacity difference ratios shown in Tables 3 and 4, it can be stated that, the effectiveness of the steel jackets in improving the residual axial load capacity of the circular columns is more significant than the square columns.

Table 3. Axial load capacity of the square columns

Model	Initial capacity (kN)	Residual capacity (kN)	Initial capacity / Residual capacity
CM1	1280	90	7%
CM2	1579	947	59.97 %
CM3	1651	1520	92 %
CM4	1930	1810	93.78 %
CM5	1910	470	26.4 %
CM6	1780	800	44.94 %

Table 4. Axial load capacity of the circular columns

Model	Initial capacity (kN)	Residual capacity (kN)	Initial capacity / Residual capacity
CD1	1380	190	13.7 %
CD2	1890	1152	61 %
CD3	2006	1885	93.96 %
CD4	2033	1900	93.45 %
CD5	2110	650	29.3%
CD6	1983	1050	52.95 %

As shown in Fig. 29, comparison between the circular and square columns indicates that the CD4 and CM4 models have almost the same residual load capacity. The circular models CD1, CD2, CD3, CD5, and CD6 had about 7, 11, 2, 15, and 11% more residual load capacity than the square models i.e., CM1, CM2, CM3, CM5, and CM6, respectively.

Accordingly, the circular model CD5 had the highest increase in the axial load capacity.

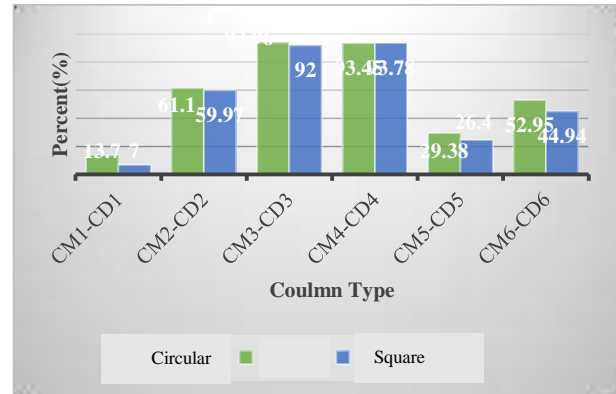


Fig. 29. Difference in the residual load capacity between the circular and square columns

4. Conclusions

In this paper, the circular and square RC column models retrofitted by a series of steel jackets were analyzed under the effects of sudden lateral loading condition using the ABAQUS/Explicit software. The main objective of this study was evaluating the efficacy of the steel jacketing on the behavior of RC columns under the impact and blast loading. The results showed that retrofitting with one-sided strips could be an effective approach to improve the axial load and explosive capacity of the RC column simultaneously. Although, retrofitting with angle steel profiles plays an essential role in enhancing the axial load capacity of the column, it is not a very effective approach for improving the lateral explosive capacity of the column. In general, strengthening, especially with steel jackets enhances the performance of the RC columns under the impact loading significantly. However, the configurations with higher buckling resistance under the gravity loading should be applied to choose the type of steel jacketing system for the RC columns. Given

the retrofitting schemes presented in this study, a full steel jacketing cannot be as effective as the one-sided steel jackets (using steel angles and channels) for reducing the column lateral deformation; Unless, its thickness increases, which is not desired in terms of structural weight and economic considerations.

One of the objectives of the present study was evaluating the effects of geometrical shape of the column on the behavior of the same steel -jacketed circular and square RC columns under the blast loading. In general, the lateral pressure wave interaction surface of the circular columns is smaller than the square columns, and the geometric shape of the circular columns causes the blast pressure waves to pass through its edges. As a result, the circular column behaves better than the square column under the same extreme loading condition. The use of steel jackets altered the behavior of the circular and square columns under the blast loading in different ways, and it is not possible to generalize the behavior of square columns to the circular ones. That is, each retrofitting system must be modeled and analyzed separately. On the other hand, the effects of $P-\delta$ should be taken into account in estimating the axial residual load capacity of the post-event columns. The reducing effect of secondary moments due to $P-\delta$ phenomenon is more significant for the square columns retrofitted by the steel jackets than the circular ones retrofitted by similar steel jackets. Increasing the compressive strength of the concrete material, as well as the percentage of longitudinal reinforcement are effective approaches in improving the column behavior against the blast loads, which is more significant in the circular columns and in the presence of a steel jacket retrofitting.

REFERENCES

- [1] Bagheripourasil, M., Mohammadi, Y. (2015). Comparison between Alternative Load Path Method and a Direct Applying Blast Loading Method in Assessment of the Progressive Collapse, *Journal of Rehabilitation in Civil Engineering*, 3(2), 1-15.
- [2] Kazemi-Moghaddam, A., Sasani, M. (2015). Progressive collapse evaluation of Murrah Federal Building following sudden loss of column G20, *Engineering Structures*, 89, 162-171.
- [3] Li, J., Hao, H. (2013). Numerical study of structural progressive collapse using substructure technique, *Engineering Structures*, 52, 101-113.
- [4] Bao, X., Li, B. (2010). Residual strength of blast damaged reinforced concrete columns, *International journal of impact engineering*, 37(3), 295-308.
- [5] Rodriguez-Nikl, T., Lee, C. S., Hegemier, G. A., Seible, F. (2012). Experimental performance of concrete columns with composite jackets under blast loading, *Journal of Structural Engineering*, 138(1), 81-89.
- [6] Fujikake, K., Aemlaor, P. (2013). Damage of reinforced concrete columns under demolition blasting, *Engineering structures*, 55, 116-125.
- [7] Crawford, J. E. (2013). State of the art for enhancing the blast resistance of reinforced concrete columns with fiber-reinforced plastic, *Canadian Journal of Civil Engineering*, 40(11), 1023-1033.
- [8] Shi, Y., Hao, H., Li, Z. X. (2008). Numerical derivation of pressure–impulse diagrams for prediction of RC column damage to blast loads, *International Journal of Impact Engineering*, 35(11), 1213-1227.
- [9] Wu, K. C., Li, B., Tsai, K. C. (2011). The effects of explosive mass ratio on residual compressive capacity of contact blast damaged composite columns, *Journal of Constructional Steel Research*, 67(4), 602-612.

- [10] Roller, C., Mayrhofer, C., Riedel, W., Thoma, K. (2013). Residual load capacity of exposed and hardened concrete columns under explosion loads, *Engineering structures*, 55, 66-72.
- [11] Aoude, H., Dagenais, F. P., Burrell, R. P., Saatcioglu, M. (2015). Behavior of ultra-high-performance fiber reinforced concrete columns under blast loading, *International Journal of Impact Engineering*, 80, 185-202.
- [12] Astarlioglu, S., Krauthammer, T. (2014). Response of normal-strength and ultra-high-performance fiber-reinforced concrete columns to idealized blast loads, *Engineering structures*, 61, 1-12.
- [13] Livermore Software Technology Corporation. (2018). LS-DYNA R11 Keyword User's Manual.
- [14] Abaqus 6.13 documentation. (2013). <http://129.97.46.200:2080/v6.13/>
- [15] Akbarzadeh Bengar, H., Yavari, M. R. (2016). Simulation of the Reactive Powder Concrete (RPC) Behavior Reinforcing with Resistant Fiber Subjected to Blast Load, *Journal of Rehabilitation in Civil Engineering*, 4(1), 63-77.
- [16] Arlery, M., Rouquand, A., Chhim, S. (2013). Numerical dynamic simulations for the prediction of damage and loss of capacity of RC column subjected to contact detonations, In: 8th International Conference on Fracture Mechanics of Concrete and Concrete Structures (FraMCoS-8), Toledo (Spain), [Online]. Accessed: <http://framcos.org/FraMCoS-8/p619.pdf>
- [17] Hyde, D. W. (1988). Microcomputer Programs CONWEP and FUNPRO, Applications of TM 5-855-1, 'Fundamentals of Protective Design for Conventional Weapons'(User's Guide) (No. WES/IR/SL-88-1), Army Engineer Waterways Experiment Station Vicksburg Ms Structures Lab.
- [18] Carriere, M., Heffernan, P. J., Wight, R. G., Braimah, A. (2009). Behavior of steel reinforced polymer (SRP) strengthened RC members under blast load, *Canadian Journal of Civil Engineering*, 36(8), 1356-1365.
- [19] He, A., Cai, J., Chen, Q. J., Liu, X., Xu, J. (2016). Behavior of steel-jacket retrofitted RC columns with preload effects, *Thin-Walled Structures*, 109, 25-39.
- [20] Jodawat, A., Parekh, A., Marathe, B., Pawar, K., Patwa, S., Sahu, Y., Jain, I. (2016). Retrofitting of Reinforced Concrete Column by Steel Jacketing, *Int. Journal of Engineering Research and Application*, 6(7), 1-5.
- [21] Crawford, J. E., Wesevich, J., Valancius, J., Reynolds, A. (1995, October). Evaluation of jacketed columns as a means to improve the resistance of conventional structures to blast effects, In *Proceedings, 66th Shock and Vibration Symposium*, Biloxi, MS (Vol. 30).
- [22] Thai, D. K., Pham, T. H., Nguyen, D. L. (2020). Investigation on the Damage of RC Columns Covered by Steel Plate under Blast Loading, *The Structural Design of Tall and Special Buildings*, (in press).
- [23] Thai, D. K., Pham, T. H., Nguyen, D. L. (2020). Damage assessment of reinforced concrete columns retrofitted by steel jacket under blast loading, *The Structural Design of Tall and Special Buildings*, 29(1), e1676.
- [24] Fouché, P., Bruneau, M., Chiarito, V. P. (2016). Modified steel-jacketed columns for combined blast and seismic retrofit of existing bridge columns, *Journal of Bridge Engineering*, 21(7), 04016035.
- [25] Fujikura, S., Bruneau, M. (2011). Experimental investigation of seismically resistant bridge piers under blast loading, *Journal of Bridge Engineering*, 16(1), 63-71.
- [26] Morrill, K. B., Crawford, M. E., Crawford, J. E., Ferritto, J. M. (2004). Retrofit of Reinforced Concrete Columns and Walls, In: *Structures Congress*, Nashville.
- [27] Tan, S. H., Poon, J. K., Chan, R., Chng, D. (2012). Retrofitting of reinforced concrete beam-column via steel jackets against close-in detonation, In: 12th international LS-DYNA users conference, 3, 1-12.
- [28] Codina, R., Ambrosini, D., de Borbón, F. (2016). Alternatives to prevent the failure of RC members under close-in blast loadings, *Engineering Failure Analysis*, 60, 96-106.

- [29] Codina, R., Ambrosini, D., de Borbón, F. (2017). New sacrificial cladding system for the reduction of blast damage in reinforced concrete structures, *International Journal of Protective Structures*, 8(2), 221-236.
- [30] Esmailnia Omran, M., Mollaei, S. (2017). Investigation of Axial Strengthened Reinforced Concrete Columns under Lateral Blast Loading, *Shock and Vibration*, 2017.
- [31] Belal, M. F., Mohamed, H. M., Morad, S. A. (2015). Behavior of reinforced concrete columns strengthened by steel jacket, *HBRC Journal*, 11(2), 201-212.
- [32] Siba, F. (2014). Near-field explosion effects on reinforced concrete columns: An experimental investigation, *Doctoral dissertation*, Carleton University.
- [33] Oliver, J., Oller, S., Oñate, E. (1989). A plastic-damage model for concrete, *International Journal of solids and structures*, 25(3).
- [34] Lee, J., Fenves, G. L. (1998). Plastic-damage model for cyclic loading of concrete structures, *Journal of engineering mechanics*, 124(8), 892-900.
- [35] Yu, T., Teng, J. G., Wong, Y. L., Dong, S. L. (2010). Finite element modeling of confined concrete-II: Plastic-damage model, *Engineering structures*, 32(3), 680-691.
- [36] FEMA (Federal Emergency Management Association). (2006). *Designer's Notebook--Blast Consideration*, FEMA Press.
- [37] U.S. Department of Defense (DOD). (2008). *Structures to Resist the Effects of Accidental Explosions*, Washington DC: UFC 3-340-02.
- [38] Gebbeken, N., Greulich, S., Pietzsch, A., Doege, T. (2003). *Interaction of Local and Global Structural Behavior of Buildings under Catastrophic Loadings, Response of Structures to Extreme Loading*, Toronto, Elsevier, 2.
- [39] Braimah, A., Contestabile, E. (2007, July). Blast Vulnerability Assessment: Challenges and Myths, In *Structures under Extreme Loading--Proceedings of First International Workshop on Performance, Protection, and Strengthening of Structures under Extreme Loading*.
- [40] Zukas, J. A., Walters, W., Walters, W. P. (Eds.). (2002). *Explosive effects and applications*, Springer Science & Business Media.
- [41] U.S. Dept. of Army, the Navy and Air Force. (1990). *The Design of Structures to Resist the Effects of Accidental Explosions*, TM 5-1300. Technical Manual, Washington DC.
- [42] Dusenberry, D. O. (2010). *Handbook for blast resistant design of buildings*, John Wiley & Sons.
- [43] Momeni, M., Hadianfard, M. A., Bedon, C., Baghlani, A. (2019). Numerical damage evaluation assessment of blast loaded steel columns with similar section properties, *Structures*, 20, 189-203.
- [44] Hadi, M. N., Widiarsa, I. B. R. (2012). Axial and flexural performance of square RC columns wrapped with CFRP under eccentric loading, *Journal of Composites for Construction*, 16(6), 640-649.
- [45] Mollaei, S. (2017). *Analysis of Reinforced Concrete Columns Subjected to Blast Loading Considering Strain Rate Effects*. PhD Thesis in Structural Engineering, University of Kurdistan.
- [46] Wu, K. C., Li, B., Tsai, K. C. (2011). Residual axial compression capacity of localized blast-damaged RC columns, *International journal of impact engineering*, 38(1), 29-40.